



Available online at [www.sciencedirect.com](http://www.sciencedirect.com)



Advances in Space Research xxx (2003) xxx–xxx

**ADVANCES IN  
SPACE  
RESEARCH**  
(a COSPAR publication)

[www.elsevier.com/locate/asr](http://www.elsevier.com/locate/asr)

## Locating landslides using multi-temporal satellite images

K.S. Cheng <sup>\*</sup>, C. Wei, S.C. Chang

*Department of Bioenvironmental Systems Engineering/Hydropack Research Institute, National Taiwan University,  
No. 1, Section 4, Taipei, Taiwan, ROC*

### 6 Abstract

Landuse/landcover change detection using remotely sensed images has been widely investigated. Most applications of this type involve either *image differencing* or *image classification* using multi-temporal images. If multi-temporal images are to be used for quantitative analysis based on their radiometric information, as in the case of change detection or landuse classification, geometric rectification and radiometric correction must be performed prior to subsequent image analyses. In particular, geometric rectification has significant effect on the accuracy of landuse change detection in areas of rugged terrain. Remote sensing image rectification is commonly done by applying a polynomial trend mapping (PTM) model to image coordinates and map coordinates of ground-control-points. A major drawback of the PTM model is that it does not capture the random characteristics of terrain elevation. In this study an ordinary kriging approach is applied for image-to-image registration. The approach considers residuals of the PTM model as anisotropic random fields and employs the ordinary kriging method for spatial interpolation of the residual random fields. Band-ratioing technique was also employed for relative radiometric normalization. From the grey-level histograms of pre- and post-event band-ratio images, we determined the percentage of landuse changes in the study area. Image differencing was then performed using the pre- and post-event band-ratio image pair. Finally, a grey-level threshold of the band-ratio difference image is determined as the value whose exceeding probability equals the areal percentage of landuse change. DTM data of the study area were also used to further restrict landslide areas to steep slope areas.

© 2003 COSPAR. Published by Elsevier Ltd. All rights reserved.

### 23 1. Introduction

Using remote sensing data and techniques for land surface change detection has gained increasing attentions in recent past. It is particularly so in Taiwan due to rapid development in hilly areas and frequent occurrences of natural disasters such as earthquakes, typhoons, and storm-induced debris flows. The ferocious Chi-Chi earthquake, that occurred on September 21, 1999 and measured at level 7.3 in Richter's scale, severely damaged several townships in Central Taiwan and drastically changed the landscape in extensive mountainous areas. After the earthquake, piled rocks and soils on the hilly areas become unstable and are vulnerable to intensive storms. As results, typhoon seasons of the following years have seen repeated occurrences of landslides and debris flows in the area claiming lives and properties of villagers. The Experi-

mental Forest of the National Taiwan University (EF-NTU) is among the most severely damaged areas. Limited by available man power, resorting to remote sensing techniques for landslide identification and restoration action planning is inevitable.

Remote sensing techniques of land surface change detection include post-classification comparison, temporal image differencing, temporal image ratioing, multifractal analysis, Bayesian probabilistic method (Lunetta and Elvidge, 1999), etc. Despite their differences in change detection algorithm, all change detection methods deal with multi-temporal images that are acquired in different dates and have different view angles, sun angles, atmospheric conditions, and spatial coverages. Therefore, a ground cell usually corresponds to different image coordinates in different images, and registration of all images to a *common reference*, be a map or a specific image, is a required pre-process for subsequent change detection. A large portion of misidentified land surface changes may occur due to inappropriate image registration. Unfortunately, many

<sup>\*</sup> Corresponding author.

E-mail address: [rslab@ntu.edu.tw](mailto:rslab@ntu.edu.tw) (K.S. Cheng).

61 applications of change detection using remote sensing  
 62 images do not pay particular attention to possible mis-  
 63 identification due to inappropriate image registration.

64 There are essentially two different categories of image  
 65 rectification/registration approaches, the deterministic  
 66 and statistical approaches. The deterministic approach,  
 67 also known as the sensor distortion model, relies on data  
 68 of the flight parameters and the terrain information, and  
 69 is effective when types of distortion are well character-  
 70 ized (Richards, 1995). For many applications, such in-  
 71 formation and parameters may not be available making  
 72 it difficult to adopt a deterministic approach of image  
 73 registration. The statistical approach, by means of a set  
 74 of ground-control-points (GCPs), establishes empirical  
 75 relationship between image coordinates and their cor-  
 76 responding map/image coordinates using standard sta-  
 77 tistical procedures. The most widely used method in this  
 78 category is the polynomial trend mapping (PTM) tech-  
 79 nique, also known as the polynomial distortion model,  
 80 that employs polynomial regression equations to relate  
 81 image coordinates and their corresponding map/image  
 82 coordinates. Although commonly applied, the PTM  
 83 technique often yields significant registration errors in  
 84 mountainous or rugged terrain areas due to its inability  
 85 to account for the local and random variation of terrain  
 86 elevation. Cheng et al. (2000) proposed an anisotropic  
 87 spatial modeling approach using ordinary kriging esti-  
 88 mation for image rectification. The approach takes into  
 89 account the spatial variation structure of terrain eleva-  
 90 tion and yields zero registration error at GCPs. It is  
 91 believed that the kriging approach can be applied for  
 92 multi-temporal image-to-image registration with high  
 93 accuracy. Therefore, the objective of this study is to  
 94 identify landslide sites with high accuracy using  
 95 multi-temporal satellite images registered by kriging  
 96 approach.

## 97 2. Study area and data

98 The Experimental Forest of National Taiwan Uni-  
 99 versity locates in Central Taiwan and covers a total area  
 100 of 333 km<sup>2</sup>. Terrain elevation in the area ranges from  
 101 220 to 3952 m above the mean sea level. A major  
 102 northerly flowing stream confluent surface runoff to the  
 103 Juo-Shuei River, one of the major rivers in Taiwan. The  
 104 area is very close to the center of the Chi-Chi earth-  
 105 quake. SPOT multi-spectral images, acquired on Octo-  
 106 ber 1, 1999 and September 21, 2001, are used in this  
 107 study for identification of landslide sites. A major ty-  
 108 phoon (Toraji) passed through the study area on July  
 109 30, 2001 and induced landslides and debris flows. Or-  
 110 thorectified airphotos of scale 1:5000 and digital terrain  
 111 model (DTM) data are also used for image rectification  
 112 and calculation of land surface slope, respectively.

## 3. Image registration and rectification

Change detection using multi-temporal images re-  
 quires all images be referenced to a common base, either  
 be a map or an image, followed by a comparison of  
 image radiances. If two images are utilized for change  
 detection two approaches may be adopted. The first  
 approach is to independently reference the two images  
 to a common Orthorectified map and then compare the  
 radiance properties of both images. The second ap-  
 proach is to firstly rectify one of the two images to an  
 Orthorectified map and then perform an image-to-image  
 registration between the two images.

The first approach will result in misidentified changes  
 owing to rectification errors on the two images and the  
 inconsistency of incorrectly rectified areas. Image-to-  
 image registration is expected to achieve higher accuracy  
 than image-to-map rectification since both images gen-  
 erally are of the same spatial resolution and have similar  
 radiance pattern making it easier to identify terrain  
 patterns and find more GCPs. This is particularly ad-  
 vantageous in this study since the earthquake has sig-  
 nificantly changed terrain features in many mountainous  
 areas, and selecting GCPs on an outdated map becomes  
 very difficult. Therefore, the second approach is adopted  
 in this study in light of achieving higher accuracy of  
 change detection through image-to-image registration.

The most widely used method for georeferencing of  
 remote sensing images is the PTM method. Let  $(x, y)$  be  
 the map or referenced-image coordinate of a pixel and  
 $(X, Y)$  be its corresponding coordinate in the distorted  
 image. Also let  $(\hat{X}, \hat{Y})$  be estimate of the image coordi-  
 nate  $(X, Y)$  by a polynomial transformation. General  
 form of the PTM algorithm is given in the following  
 equation:

$$\hat{X} = \sum_{i=0}^n \sum_{j=0}^i a_{ij} x^{i-j} y^j, \quad (1a)$$

$$\hat{Y} = \sum_{i=0}^n \sum_{j=0}^i b_{ij} x^{i-j} y^j. \quad (1b)$$

Here  $n$  is the order of the polynomial model and the  
 coefficients  $a_{ij}$  and  $b_{ij}$  are estimated by least-squares re-  
 gression analysis. The PTM is basically a statistical  
 trend surface mapping model. Using a set of  $m$  GCPs,  
 $[(x_k, y_k); (X_k, Y_k)]$ ,  $k = 1, 2, \dots, m$ , it finds the best-fit  
 surface for the GCP data set. Low-order polynomials  
 are used to rectify images with less geometric distor-  
 tions, like satellite images from a flat region. Geometric  
 distortions like scale, translation, rotation, and skew  
 effects can be modeled by an affine transformation  
 $(n = 1)$ . Therefore, the affine transformation can be used  
 for approximate correction of satellite sensor- and orbit-  
 related distortions. Application of the PTM technique to  
 image rectification in areas with significant variation of

163 terrain elevation requires using higher order polynomi-  
 164 als and often leads to significant image distortions for  
 165 regions outside the range of GCPs. Since image rectifi-  
 166 cation in the PTM technique is based on the least  
 167 squares regression, it does not account for the effect of  
 168 local terrain variation on rectification accuracy, and  
 169 inevitably yields rectification errors at all GCPs.

170 Cheng et al. (2000) proposed a geostatistical ap-  
 171 proach of image rectification that takes into account  
 172 the effect of terrain variation on rectification accuracy  
 173 and yields zero rectification error at all GCPs. The  
 174 approach assumes that the spatial distribution of  
 175 registration errors resulted from a low-order PTM  
 176 model can be modeled as a random field which may  
 177 be isotropic or anisotropic. Spatial variation structure  
 178 of such a random field is then characterized by a  
 179 variogram, and estimation of PTM-based registration  
 180 errors at non-GCP locations are estimated by ordinary  
 181 kriging. Finally, the estimated registration errors are  
 182 added to the PTM estimates  $(\hat{X}, \hat{Y})$  to yield the final  
 183 rectified coordinates. Detailed theory of kriging esti-  
 184 mation can be found in Journel and Huijbregts (1978)  
 185 and Chilès and Delfiner (1999).

186 Procedures of ordinary kriging approach of image-to-  
 187 image registration are as follows:

- 188 (1) Select a set of GCPs using multi-temporal images.
- 189 (2) Perform the first order PTM to establish trend rela-  
 190 tionship between image coordinates of the two im-  
 191 ages.
- 192 (3) Consider the registration errors in E-W and N-S di-  
 193 rections as two residual random fields and separately  
 194 perform the anisotropic variogram modeling for  
 195 each random field.
- 196 (4) Apply the ordinary kriging estimation to the residual  
 197 random fields using anisotropic variograms estab-  
 198 lished in step (3).
- 199 (5) Final result of the image-to-image registration is  
 200 obtained by adding ordinary kriging estimates of  
 201 the residual fields to the trend field estimated by  
 202 PTM.

203 The ordinary kriging approach of image registra-  
 204 tion/rectification has the advantage of capturing local  
 205 terrain variation and reducing the image distortion  
 206 caused by terrain variation. Particularly, in the case of  
 207 image-to-image registration for multi-temporal images  
 208 of the same spatial resolution, many GCPs scattering  
 209 around the study area can be used, and the fact of  
 210 zero registration error at all GCPs guarantees better  
 211 overall registration accuracy. Readers are referred to  
 212 Cheng et al. (2000) for a complete description of the  
 213 approach. Image-to-map rectification can be done in a  
 214 similar way except that map coordinates are involved.  
 215 Fig. 1 shows result of the image-to-image registration  
 216 by ordinary kriging approach for a portion of the  
 217 study area.

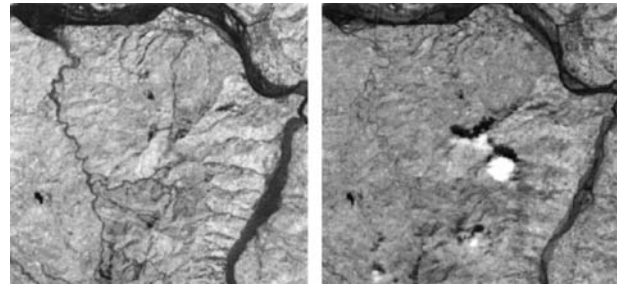


Fig. 1. IR band image pair after image-to-image registration.

## 4. Change detection 218

### 4.1. Spectral ratioing 219

220 Since multi-temporal images have different atmo-  
 221 spheric conditions, spectral ratioing analysis is per-  
 222 formed to effectively compensate for brightness  
 223 variation caused by different atmospheric conditions. It  
 224 can be seen in Fig. 1 that IR band brightness of the pre-  
 225 typhoon image is lower than that of the post-typhoon  
 226 image. After the IR/R band-ratioing, brightness values  
 227 of the two band-ratio images are very close, as can be  
 228 seen in Fig. 2.

### 4.2. Spectral histogram peaks matching 229

230 Both spectral histograms of the pre- and post-ty-  
 231 phoon band-ratio images have two correspondent  
 232 peaks. Peaks in the histogram represent major landuse/  
 233 landcover types and they should have stable grey levels  
 234 in multi-temporal band-ratio images. The histogram  
 235 stretch technique was implemented to match corre-  
 236 spondent histogram peaks. Fig. 3 shows spectral histo-  
 237 grams of band-ratio images after histogram peaks  
 238 matching.

### 4.3. Estimating percentage of changed areas 239

240 The histogram peaks matching yields pre- and post-  
 241 event IR/R band-ratio images that have stable grey-level  
 242 values for major landuse/landcover types. However,  
 243 frequencies of specific grey levels are different in the two  
 244 images. Frequency difference implies the number of  
 245 pixels corresponding to landuse/landcover changes. Let  
 246  $f_1(g)$  and  $f_2(g)$ , respectively, represent the frequency of  
 247 grey level  $g$  in pre- and post-event IR/R band-ratio  
 248 images. The total number of pixels associated with  
 249 landuse/landcover changes,  $N_C$ , and percentage of  
 250 changed areas,  $p$ , are then estimated by the following  
 251 equations:

$$N_C = \frac{1}{2} \sum_{g=1}^{256} |f_1(g) - f_2(g)|, \quad (2)$$

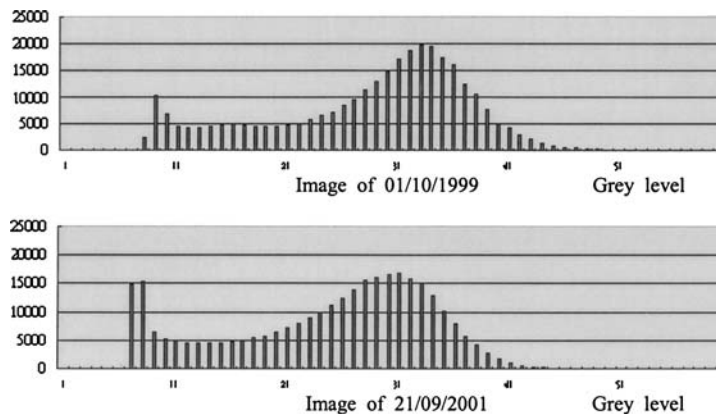


Fig. 2. Spectral histograms of IR/R band-ratio images.

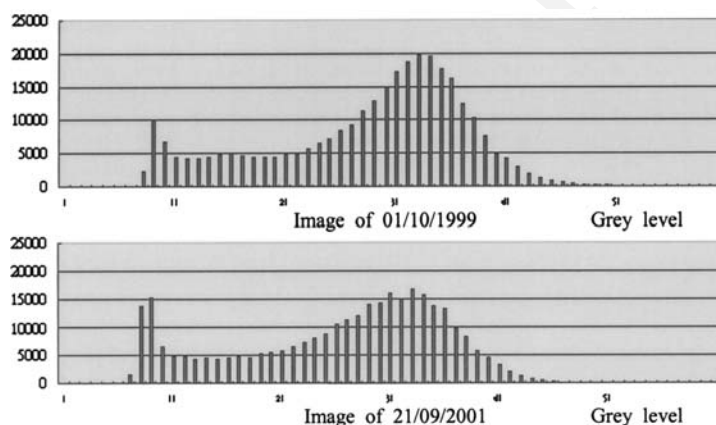


Fig. 3. Spectral histograms of IR/R band-ratio images after histogram peaks matching.

$$p = 100(N_C/N), \quad (3)$$

254 where  $N$  is the total number of pixels in the image.  
 255 Multiplying with  $1/2$  in Eq. (2) is to avoid double  
 256 counting of the number of changed pixels.

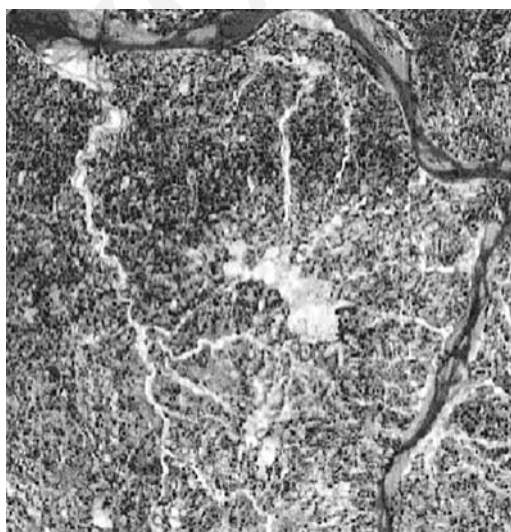


Fig. 4. IR/R band-ratio difference image.

#### 4.4. Determining a threshold for change detection

257

258 Occurrences of landcover change correspond to sig-  
 259 nificant difference in grey-level values of the pre- and  
 260 post-event IR/R images. Therefore, multi-temporal im-  
 261 age differencing was implemented using pre- and post-  
 262 event IR/R band-ratio images to yield an IR/R band-  
 263 ratio difference image (see Fig. 4), hereafter referred to  
 264 as the difference image. Grey level of pixels in the dif-  
 265 ference image,  $g_{diff}$ , is calculated by

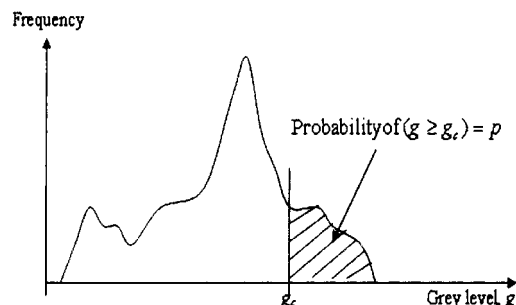


Fig. 5. Illustrative grey-level histogram of the difference image.

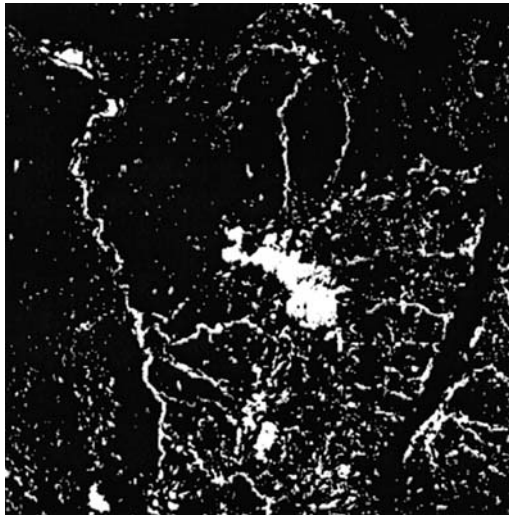


Fig. 6. Identified landcover-changed areas.

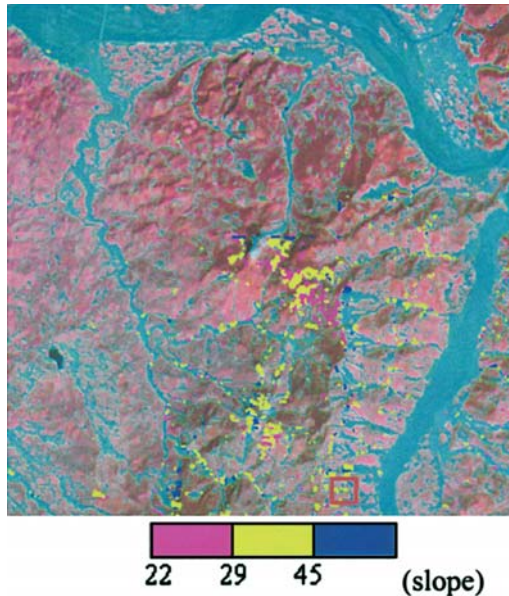


Fig. 7. Identified landslide sites.



(a)



(b)

Fig. 8. Airphotos taken before and after Typhoon Toraji of an identified landslide site.

$$g_{\text{diff}} = |g_{\text{pre}} - g_{\text{post}}|, \quad (4)$$

where  $g_{\text{pre}}$  and  $g_{\text{post}}$  are grey levels in the pre- and post-event band-ratio image, respectively. In the difference image, pixels associated with landcover changes have higher grey levels. A grey-level threshold,  $g_c$ , for change detection using the difference image, is determined by locating the grey level whose exceeding probability equals the areal percentage of landuse changes,  $p$ , as depicted in Fig. 5. Changed areas identified by the grey-level threshold  $g_c$  are shown in Fig. 6 (white areas). Since not all change-detected areas are landslide sites, DTM data were used to generate a slope image of the study area and landslide identification is restricted to the area with slope steeper than  $22^\circ$ . Using  $22^\circ$  as an empirical threshold for identifying landslides is based on previous studies of slopes of landslide sites in a Taiwan's watershed. Fig. 7 shows the identified landslide sites in the study area. Many identified landslide sites have been verified by field investigations and high resolution airphotos. For example, Fig. 8 shows the airphotos taken before and after the occurrence of Typhoon Toraji of an identified landslide site corresponding to the red blocked area in Fig. 7. It can be seen clearly that landslide occurred in a large area on the left half of Fig. 8(a) after Typhoon Toraji. Also, the large white cluster near the center in Fig. 6 represents a cloud covered area and therefore identified landslides in this region must be excluded. Although the threshold value is adopted to ensure high accuracy of identified landslides; however, it is also recognized that landslides may occur in lower slope areas.

## 5. Conclusion

In this study we demonstrate that the ordinary kriging approach of image-to-image registration yields

300 high registration accuracy in mountainous and rugged  
301 terrain areas. The spectral ratioing technique yields  
302 similar brightness values for multi-temporal SPOT  
303 images and these multi-temporal band-ratio images  
304 can be used to estimate the percentage of landcover  
305 changes in the study area. The multi-temporal image  
306 differencing technique yields a band-ratio difference  
307 image which can be used to determine the grey-level  
308 threshold for change detection. It is also demonstrated  
309 in this study that DTM data are very valuable in  
310 extracting landslide sites from the detected landcover-  
311 changed areas.

### 312 Acknowledgements

313 The authors are grateful for the financial support of a  
314 project by the Council of Agriculture of Republic of  
315 China. Special thanks are also given to staff members of

the Experimental Forest of National Taiwan University, 316  
in particular, Professor Y.N. Wang. We also acknowl- 317  
edge the constructive comments and suggestions pro- 318  
vided by reviewers. 319

### References 320

- Cheng, K.S., Yeh, H.C., Tsai, C.H. An anisotropic spatial modeling 321  
approach for remote sensing image rectification. *Remote Sens.* 322  
*Environ.* 73 (1), 46–54, 2000. 323
- Chilès, J.P., Delfiner, P. *Geostatistics – Modeling Spatial Uncertainty.* 324  
Wiley, New York, pp. 449–451, 1999. 325
- Journel, A.G., Huijbregts, C.J. *Mining Geostatistics.* Academic Press, 326  
London, 600 p, 1978. 327
- Lunetta, R.S., Elvidge, C.D. *Remote Sensing Change Detection.* 328  
Taylor & Francis Ltd., London, 318 p, 1999. 329
- Richards, J.A. *Remote Sensing Digital Image Analysis.* Springer, 330  
Berlin, pp. 54–57, 1995. 331